Scientific paper

Zinc(II) Complex Containing Oxazole Ring: Synthesis, Crystal Structure, Characterization, DFT Calculations, and Hirshfeld Surface Analysis

Karwan Omer Ali,[1,*] Hikmat Ali Mohamad,[2] Thomas Gerber[3] and Eric Hosten[3]

[1] *Department of Physics, College of Science, University of Halabja, Halabja 46018, Iraq*

[2] *Department of Chemistry, College of Education, Salahaddin University, Erbil 44001, Iraq*

[3] *Department of Chemistry, Faculty of Science, Nelson Mandela University, Port Elizabeth 6031, South Africa*

* *Corresponding author: E-mail: karwan.ali@uoh.edu.iq*
Phone No. 009647503849284

Received: 07-12-2022

Abstract

A new complex of Zn(II), with 5-chloro-2-methylbenzoxazole ligand (L), has been synthesized by the reaction of zinc dichloride with the ligand (L= C_8H_6ClNO) in ethanol solution: dichloridobis(5-chloro-2-methyl-1,3-benzoxazole)-zinc(II), $C_{16}H_{12}Cl_4N_2O_2Zn$. The synthesized complex has been fully characterized by elemental analysis, molar conductivity, FT-IR, UV-Vis, and single-crystal X-ray diffraction (XRD). The XRD analysis reveals that the complex has a 1:2 metal-to-ligand ratio. The zinc(II) complex has a distorted tetrahedral geometry with two coordinated nitrogen atoms from the ligand. Density Functional Theory (DFT) calculations were performed at the B3LYP level of theory using the LANL2DZ basis set for metal complex and the 6–31G(d) basis set for non-metal elements to determine the optimum geometry structure of the complex, and the calculated HOMO and LUMO orbital energies were presented. A natural bond orbital (NBO) analysis was carried out on the molecules to analyze the atomic charge distribution before and after the complexation of the ligand. The Hirshfeld surface mapped over d_{norm}, shape index, and curvature exhibited strong H...Cl/Cl...H and H...H intermolecular interactions as the principal contributors to crystal packing.

Keywords: Zn(II), Benzoxazole, Distorted tetrahedral geometry, Hirshfeld surface analysis, NBO analysis, DFT calculations

1. Introduction

Benzoxazole is a bicyclic heterocyclic compound containing both oxygen and nitrogen atoms in which the benzene ring is fused to a 1,3-oxazole ring at positions 4 and 5.[1] It is one of the most common heterocyclics in industry and scientific research.[2] Transition metal ions have different binding forces with N and O atoms.[3] Commonly, N-donor oxazole groups have demonstrated excellent coordination ability with the first-row transition metal ions.[4] Due to the variety of coordination modes and configurations, N-heterocyclic ligands are typically used as neutral ligands in the synthesis of metal complexes.[5,6] Counterions are used to balance the total charge when studying the neutral ligand, which not only affects the coordination modes of the metal ions but also the entire geometry of the metal complex.[7,8] Most Zn(II) complexes show tetrahedral and distorted tetrahedral coordination geometries, in agreement with a d^{10} electronic configuration.[9,10] Thus, the strategy of using neutral mono and bidentate ligands with metal halides to force tetrahedral geometry has been widely used for stabilizing Zn(II) complexes. Similarly, benzoxazole derivatives have also been used to stabilize zinc in a +2 oxidation state.[11] Because of their good emission properties and inexpensive cost compared to other d^{10} metal complexes, zinc (II) complexes have been shown to be important candidates for electroluminescent applications. For example, the Zinc(II) complex of [(2-(2-hydroxyphenyl)benzoxazole)(2-methyl-8-hydroxyquinoline)] has been recognized as a blue-emitting zinc complex to fabricate stacked organic light-emitting diodes.[12] Changes in the intermolecular interactions between metal ions and ligands that are

studied by the Hirshfeld surface analysis and DFT calculations can be seen in a series of Zinc(II) complexes with 2-(4-imidazolyl)-4-methyl-1,2-quinazoline-N^3-oxide,[13] 2-cetylpyridinenicotinichydrazone,[14] and sulfamethoxazole,[15] etc. Nonetheless, data on X-ray crystal structures and theoretical studies of related complexes containing an oxazole ring are scarce. The current work reports the synthesis and characterization of a new zinc(II) complex based on a 5-chloro-2-methylbenzoxazole ligand (L), which was characterized by elemental analysis, molar conductivity, FT-IR, UV-Vis, and X-ray analysis. Furthermore, the crystal structure was verified using Hirshfeld surface analysis, and it is helpful for understanding the intermolecular forces in crystal packing. In addition, DFT calculations were done to predict the electronic and geometrical structure of the complex.

2. Experimental

2. 1. Materials and General Methods

The solvents used in this study (Ethanol 99% and dimethyl sulfoxide 99.8%) were purchased from Alfa Aesar and used without further purification. 5-Chloro-2-methylbenzoxazole produced by Sigma Aldrich was used without purification. Single-crystal X-ray structure measurement was performed at 200 K using a Bruker Kappa Apex II diffractometer with a radiation wavelength of (λ = 0.71073 Å). C, H, N, and O percentages were determined by EURO EA 300 CHNS analyzer. A Shimadzu FT-IR-8400S spectrophotometer was used to record infrared spectra in the 4000–400 cm^{-1} range as KBr discs and the 600–200 cm^{-1} range as CsI discs. The UV–visible spectra in DMSO were measured on the AEUV1609 LTD Shimadzu spectrophotometer. The molar conductivities were measured on Meter CON 700 Benchtop conductivity meter using 10^{-3} M solutions of the complex and ligands in DMSO at room temperature. The melting point was measured using scientific Stuart SMP3 melting point equipment.

2. 2. Synthesis of *[Zn(L)$_2$Cl$_2$]*

A solution of $ZnCl_2$ (0.284 g, 2.0 mmol) in ethanol (25 mL) was added dropwise under stirring to a solution of 5-chloro-2-methylbenzoxazole (L=C_8H_6ClNO) ligand (0.670 g, 4.0 mmol) in ethanol (25 mL). Subsequently, the mixture was stirred for 5 hrs. at room temperature with the formation of a clear solution, which was then evaporated slowly at room temperature to yield pale-yellow crystalline products within one week. m.p. 208–209 °C. Yield: 0.915 g (96%). Anal. Calcd. for $C_{16}H_{12}Cl_4N_2O_2Zn$: C 41.10, H 2.56, N 5.94, O 6.78. Found: C 41.05, H 2.70, N 5.97, O 6.79. Molar conductivity: 9.11×10^{-5} S cm^2 mol^{-1}. FT-IR (KBr) 3091, 3062, 1600, 1562, 1452, 1303, 445, 343 cm^{-1}. UV–Vis data in DMSO [λ/nm, (cm^{-1})]: 426(23474), 287(34843), 280(35714).

2. 3. X-ray Crystal Structure Determination

X-ray diffraction measurement for the Zn(II) complex was performed on a Bruker Kappa Apex II X-ray diffractometer equipped with graphite monochromated Mo-Ka radiation (λ = 0.71073 Å) at 200 K. The structure was solved by a dual-space algorithm using SHELXT-2018 and refined by least-squares procedures using the SHELXL-2018/3 crystallographic software.[16,17] All C, N, Cl, O, and Zn atoms were anisotropically resolved. The hydrogen atoms attached to C atoms were allowed to rotate geometrically and treated as a riding model with a C-H distance of 0.95 Å (aromatic) and 0.98 Å (-CH_3 group) with U_{iso}(H) = 1.2 U_{eq}(C).[18] The crystal data and structure refinement details for the complex are summarized in (Table 1).

Table 1. Crystal data and structure refinement of the complex

Formula	**$C_{16}H_{12}Cl_4N_2O_2Zn$**
Formula weight	471.47
Temperature, K	200
Wavelength, nm	0.71073
Crystal system	Monoclinic
Space group	$P2_1/n$
Crystal size, mm	0.52 × 0.53 × 0.67
a / Å	7.5590(5)
b / Å	7.1873(5)
c / Å	33.842(2)
α / °	90
β / °	95.101(3)
γ / °	90
V / Å^3	1831.3(2)
Z	4
D_c / g cm^{-3}	1.710
Absorption coefficient, mm^{-1}	1.937
θ range for data collection, °	2.4, 28.3
Dataset	–10:9; –9:9; –43:45
F_{000}	944
No. of reflections	4539
No. of parameters	228
R_{int}	0.027
R_1, wR_2	0.0405, 0.0921
S	1.28
[$I > 2\sigma(I)$]	4325
$\Delta\rho_{min}$, $\Delta\rho_{max}$ / eÅ^{-3}	–0.83, 0.47

2. 4. Computational Details

To better understand the structure of the zinc complex, the Gaussian 09 software package was used for density functional theory (DFT) calculations. The frontier molecular orbitals of the ligand and the Zn(II) complex were helped by the Gauss View 6.0 software at the B3LYP level of theory. In particular, the LANL2DZ basis set for the zinc metal atom[19] and the 6-31G(d)[20] basis set for

non-metal elements (C, H, N, O, and Cl) were both treated. The neutral bond orbital (NBO) analysis of the complex was done using the Gaussian 09 program at the same level of theory.[21]

2. 5. Hirshfeld Surface

A crystallographic information file (CIF) obtained from single-crystal X-ray diffraction analysis was used as an input file for Hirshfeld surface visualization of the zinc complex. To generate the Hirshfeld surface analysis and a better understanding of the intermolecular interactions in the complex crystal structure, the program Crystal Explorer 21.5 was used.[22] Hirshfeld surface visualization, presentation of results as d_{norm}, shape index, and curvedness, and calculation of 2D fingerprint plots with dean d_e and d_i distances were produced using the same software.[23]

4. Results and Discussion

The zinc (II) complex is formed by the complexation of Zn(II) chloride with the 5-chloro-2-methylbenzoxazole ligand, as shown in (Scheme 1). The complex is stable under atmospheric conditions. The complex was produced as pale-yellow crystals at a good yield suitable for single-crystal X-ray structure analysis. At room temperature, the complex is soluble in common organic solvents such as dimethyl sulfoxide, dimethylformamide, and chloroform, but not in ethanol, acetone, methanol, and petroleum ether.

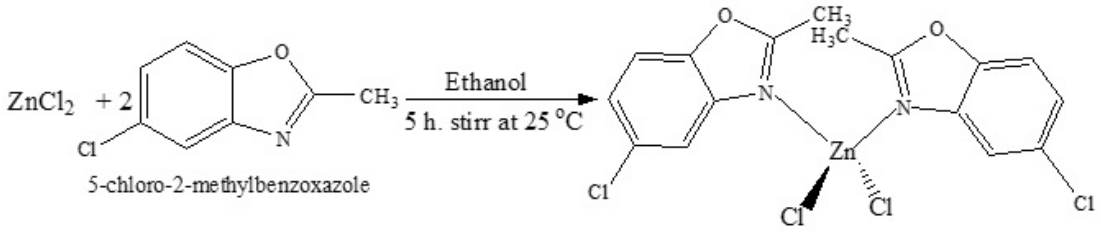

Scheme 1. Synthetic route of the Zn(II) complex.

3. 1. The Crystal Structure Description of the Zn(II) Complex

The crystal molecular structure of the $[Zn(L)_2(Cl)_2]$ complex was depicted in (Figure 1). Relevant bond lengths and bond angles from X-ray diffraction are summarized in (Table 2). Through two nitrogen atoms from the oxazole ring and two chlorine atoms, the Zn(II) metal is located on a crystal lattice center and achieves a slightly distorted tetrahedral coordination geometry. Bond angles of the internal coordination sphere of the complex, which are different from the ideal angle of 109° for a perfect tetrahedral geometry, are [(Cl3-Zn1-Cl4) 120.52(3)°, (Cl3-Zn1-N1) 108.88(7)°, (Cl3-Zn1-N2) 104.79(7)°, (Cl4-Zn1-N2) 109.70(8)°, and (Cl4-Zn1-N1) 104.99(7)°]. The Zn-Cl bond distances range between 2.1986(7) and 2.2799(14) Å, and the bond angles involving the Zn(II) atom range between 97.5(13)° and 114.87(11)° are comparable to those found in the literature.[24,25] The bond distances between Zn1-N1 (2.068(3)) and Zn1-N2 (2.042(3)) are shorter than those between Zn1-Cl3 (2.2154(9)) and (Zn-Cl4 2.2227(9)), indicating that the interaction between Zn(II) metal center and N atom is stronger than that between Zn(II) and Cl atom. The Torsion/Dihedral Angles of N2-Zn1-N1-C17, N1-Zn1-N2-C27, Cl4-Zn1-N1-C11, and Zn1-N2-C21-C26 are 63.0(3)°, 48.9(3)°, 111.0(2)°, and 6.7(5)° respectively, which results in a steric interaction between methyl groups on the benzoxazole rings and electron repulsion of chlorine atoms.[26] Consequently, crystallographically generated centroids Cg(1) to Cg(4) were related to the various aromatic rings around the Zn(II) centers. The distance between the adjacent ring centroids for Cg(1)···Cg(1), Cg(2)···Cg(2), Cg(3)···Cg(3), and Cg(4)···Cg(4) are 4.7676(17), 4.5328(18), 5.4387(19), and 3.7652(18) Å respectively. As shown in Figure 1, the electron density around C18 clearly shows that this methyl group has the rotational disorder, whereas C28 has not. Each hydrogen for the C18 group has half occupancy, so the total number of hydrogens is three.

Table 2. Selected bond distances (Å) and bond angles (°) of the complex.

Zn1-Cl3	2.2154(9)	Cl3-Zn1-Cl4	120.52(3)
Zn1-Cl4	2.2227(9)	Cl3-Zn1-N1	108.88(7)
Zn1-N1	2.068(3)	Cl3-Zn1-N2	104.79(7)
Zn1-N2	2.042(3)	Cl4-Zn1-N1	104.99(7)
N1-C11	1.421(4)	Cl4-Zn1-N2	109.70(8)
N1-C17	1.302(4)	N1-Zn1-N2	107.41(11)
N2-C21	1.412(4)	C12-O1-C17	105.0(2)

3. 2. FT-IR Spectra

In the free ligand (Fig. S1), the bands at 3093 cm^{-1} and 1166 cm^{-1} are attributed to C-H and C-Cl stretching vibrations, respectively.[27] Free 5-chloro-2-methylbenzoxazole shows strong intensity bands at 1608 cm^{-1} and 1253 cm^{-1}, with the two bands being assigned to the C=N and

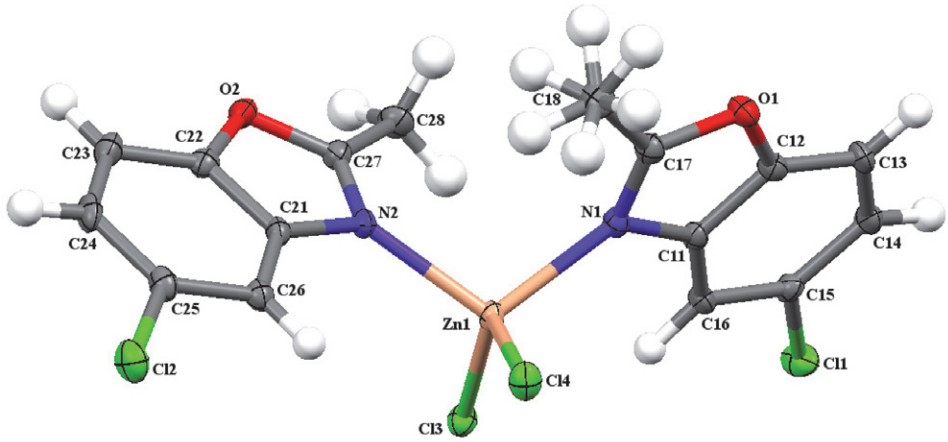

Figure 1. Single-crystal x-ray molecular structure of the complex. ellipsoids with a 30% of probability

C-O stretching vibrations of the oxazole group, respectively.[28,29] The C=N band in the Zn(II) complex (Fig. S2) is shifted to lower wavenumber (1600 cm^{-1}) indicating the participation of benzoxazole nitrogen in coordination with the Zn(II) ion.[30] The presence of a new weak band at 445 cm^{-1} in the spectrum of the complex corresponding to the (Zn-N) vibration band also confirms the bonding between ligand and Zinc metal.[31] In the IR spectrum of the zinc complex (Fig. S3), the weak band at 343 cm^{-1} was matching to Zn-Cl vibration.[32]

3. 3. Electronic Spectra and Conductivity Properties

The electronic absorption spectra of 5-chloro-2-methylbenzoxazole (L) Ligand and their complex were measured at room temperature in 10^{-3} mol. L^{-1} DMSO solution (Figure 2). The free ligand 5-chloro-2-methylbenzoxazole shows high energy absorption bands at 280 and 287 nm, which are attributed to ligand π–π* transitions of the benzene ring and C=N bond respectively.[33,34] These absorption bands that remain unchanged in the spectrum of the complex indicate the coordination of the ligand to the Zn(II) metal center. Additionally, a new absorption peak in the complex was observed at 426 nm (23474 cm^{-1}), which is attributed to the ligand-to-metal charge transfer (LMCT) that is characteristic of the zinc metal complex.[35] The synthesized complex containing chlorinated ligand had a very low molar conductivity value in DMSO (9.11 10^{-5} S. cm^2. mol^{-1}), showing that it is non-electrolyte in nature.[36]

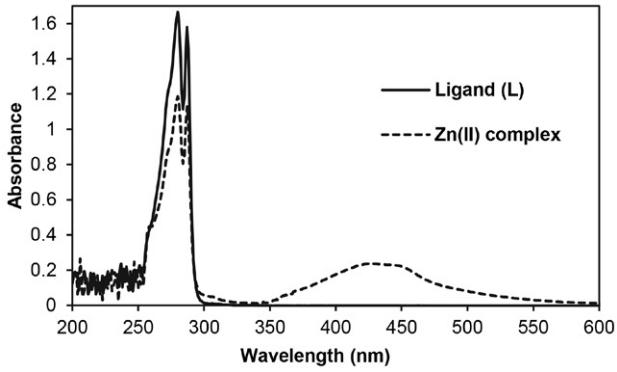

Figure 2. Electronic absorption spectra of ligand (L) and Zn(II) complex

3. 4. DFT Studies

The frontier molecular orbitals were used to investigate the electronic properties of the ligand (L) and complex. The energies of the highest occupied molecular orbital (E_{HOMO}) and the lowest unoccupied molecular orbital (E_{LUMO}) are used to estimate the HOMO-LUMO energy gap ($\Delta E = E_{LUMO-} E_{HOMO}$). The E_{HOMO}, E_{LUMO}, and ΔE energy gaps of the ligand and Zn(II)complex are shown in (Table 3) and (Figure 3). The free 5-chloro-2-methylbenzoxazole ligand has an energy gap (ΔE) of 3.526 eV, while the Zn(II) complex has an ΔE of 2.423 eV. According to DFT calculations, Beheshti et al. reported the synthesis of a pyrazolyl-based mononuclear zinc(II) complex with a 4.59 eV HOMO-LUMO energy gap.[37] The HOMO-LUMO energy gap value of the zinc(II) complex based on the benzoyl hydrazone ligand was calculated by the DFT method to be 3.76 eV in 2017.[38] As a result, the synthesized zinc(II) complex in this study is less stable than those that have been previously described. The HOMO orbital primarily acts as an electron donor, whereas the LUMO orbital mainly acts as an electron acceptor. A metal complex that has a large HOMO-LUMO energy gap is more stable than one that has a small HOMO-LUMO energy gap. The calculated NBO atomic charges of atoms for the free ligand and its complex are collected in Table 3. The calculated charge on the zinc metal (+0.993) is lower than the formal charge of the zinc ion (+2), suggesting electron transfer from the ligand to the metal center.[39] The NBO data shows that the N2 atom in the complex has a greater negative charge than the N1 atom. This result supports X-ray results showing

the Zn1-N2 bond distance is shorter than the Zn1-N1 bond distance and suggests that N2 is coordinated to the metal center more strongly than N1.[40]

Table 3. HOMO-LUMO orbital energies (eV) and NBO Charges (e) of ligand (L) and its complex

Parameter	Ligand		Zn complex
E_{HOMO}	–5.672		–6.381
E_{LUMO}	–2.146		–3.958
ΔE	3.526		2.423
The NBO charge of ligand and Zin(II) complex			
Atom	**Ligand**	**Atom**	**Zn complex**
Cl	0.009	Zn	0.993
N	–0.541	Cl4	–0.608
O	–0.505	Cl3	–0.605
		N1	–0.697
		N2	–0.737

3. 5. Hirshfeld Surfaces Analysis (HAS)

The Hirshfeld surface analyses (HSA) and the fingerprints of the zinc complex were achieved with Crystal Explorer 21.5 program.[22] Fingerprint plots of the complex is displayed in (Figure 4). Similarly, Hirshfeld surface (HS) of the complex is shown in (Figure 5). Figure 5 exposes surfaces that were mapped across d_{norm}, shape index, and curvature. The d_{norm} surface has been mapped over a range of –0.0490 to 1.3232 Å while shape index and curvedness are mapped over the ranges –1.0000 to 1.0000 Å and –4.0000 to 0.4000 Å, respectively. As illustrated in (Figure 4), the 2D fingerprint plots reveal that the major intermolecular interactions in the zinc complex are H...Cl/Cl...H, H...H, H...C/C...H, C...Cl/Cl...C, C...O/O...C, C...C, H...O/O...H, and O…Cl/Cl...O. The highest contribution to the overall Hirshfeld surface occurs due to H…Cl/Cl...H close contacts with 39.1%. The percentages of H...H, H...C/C...H, C...Cl/Cl...C, C...O/O...C, C...C, H...O/O...H, O..Cl/Cl...O, Cl…Cl, H…N/N…H, C…N/N…C, Zn…H/H…Zn, and Cl…N/N…Cl interactions are 21.7, 7.7, 7.0, 5.7, 4.7, 4.8, 3.4, 3.4, 1.8, 0.3, 0.3, and 0.1 % of the complex surface, respectively. The d_{norm} Hirshfeld surface of the complex shows red and white spots, which indicate the presence of C-H...Cl and C-H..H intermolecular interaction in the crystal structure of the zinc complex respectively. The shape index and curvedness of HS can be used to investigate π···π stacking interaction, where blue triangles represent convex regions of the compound inside the surface and red triangles represent concave regions above the

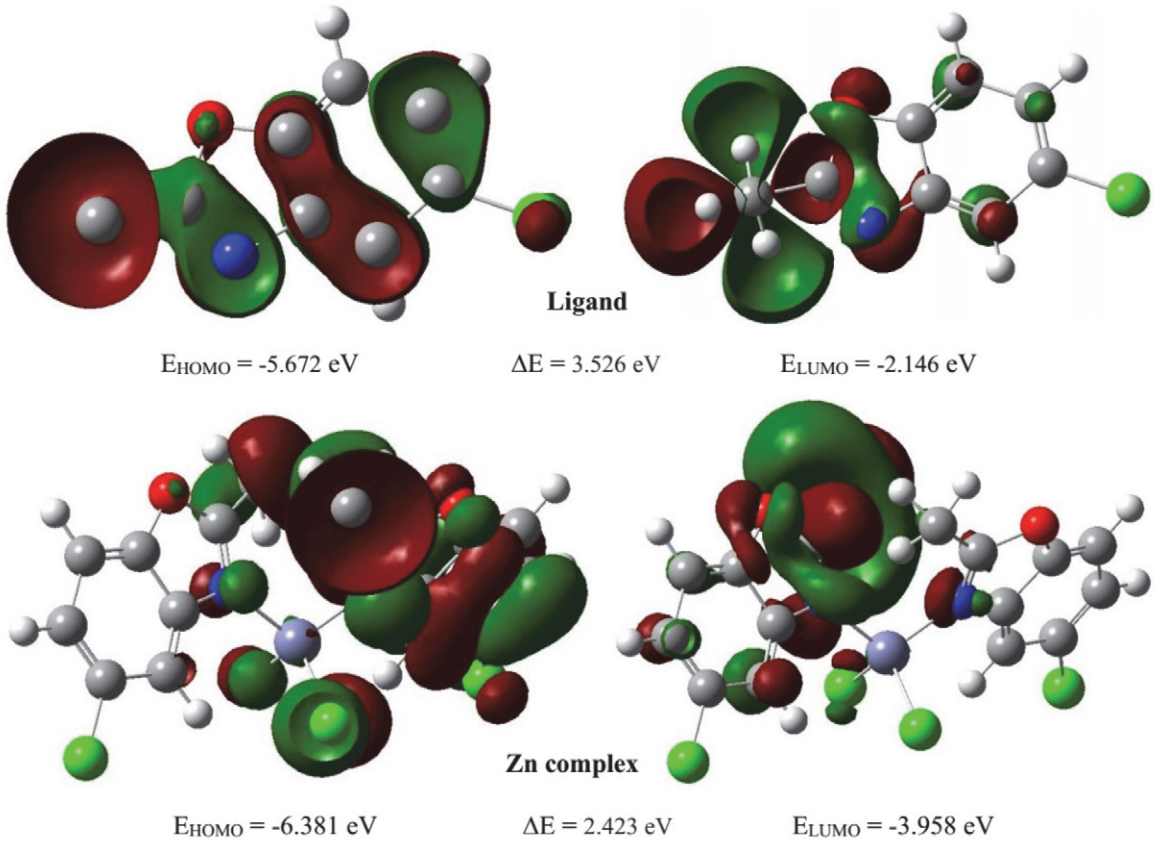

Figure 3. Surface plots of HOMO and LUMO orbitals of ligand (L) and zinc complex

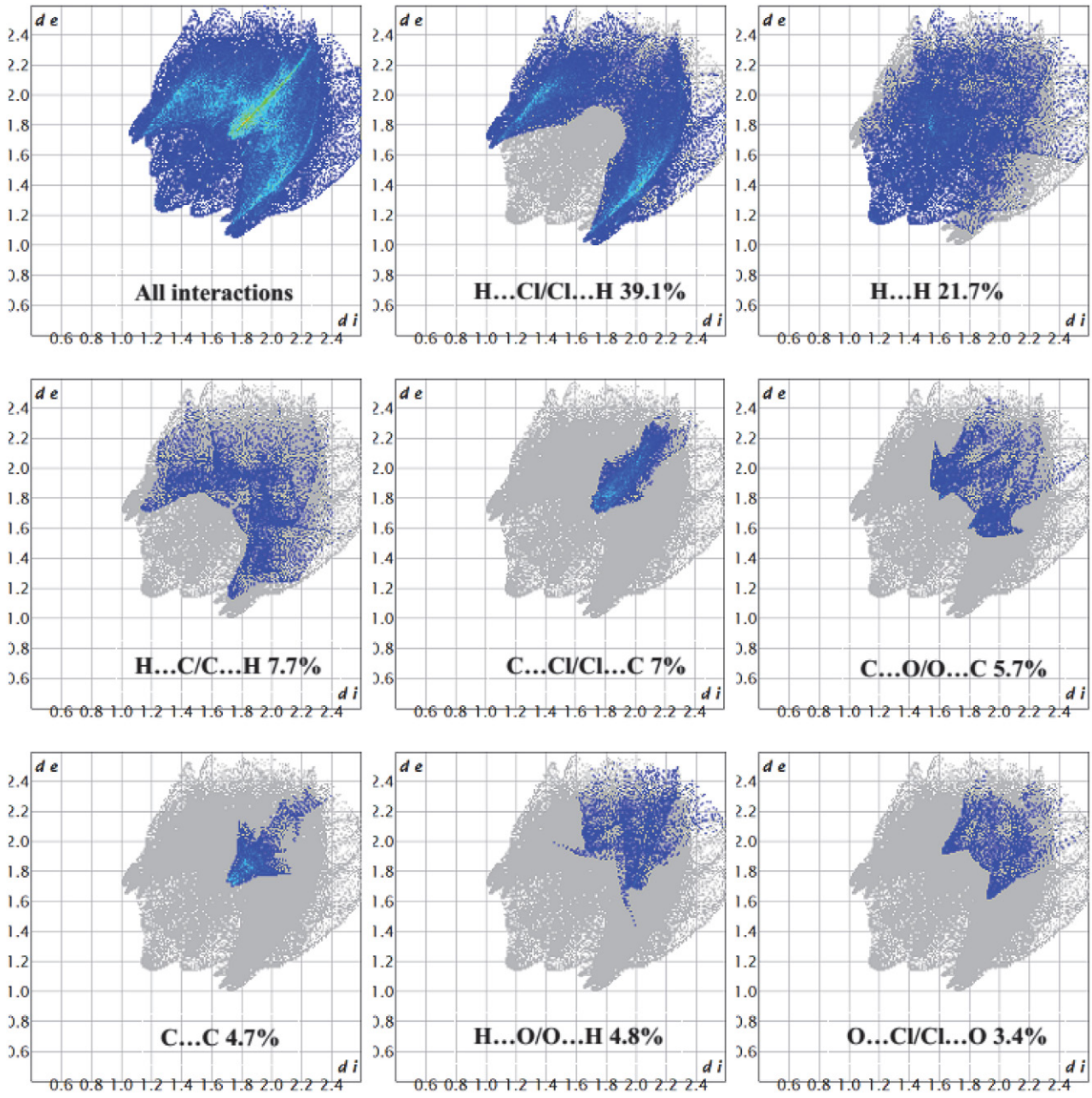

Figure 4: Fingerprint plots for the zinc(II) complex show the percentages of major contacts contributed to the total Hirshfeld surface analysis (HAS).

surface due to the π···π stacked compound's phenyl carbon atoms.[41] Green flat regions on the curvedness surface also indicate the presence of π···π interaction in the complex.

4. Conclusion

In summary, a new zinc(II) complex was synthesized with a 5-chloro-2-methylbenzoxazole ligand. The spectroscopic method and crystallographic data indicated the formation of a mononuclear zinc complex with a benzoxazole ligand acting as a monodentate ligand in neutral form. Structural analysis showed a tetracoordinate environment via two nitrogen and two chloride anions of the complex with distorted tetrahedral geometry. The electronic spectrum of the complex displayed a peak at 23474 cm^{-1}, which corresponded to the ligand-to-metal charge transfer (LMCT). The DFT study reveals that the zinc complex was less stable and more reactive than the ligand. The NBO analysis showed that the charge on the zinc metal surrounded by the nitrogen atoms of the ligand is 0.993 e found to be lower than the formal charge of the zinc ion

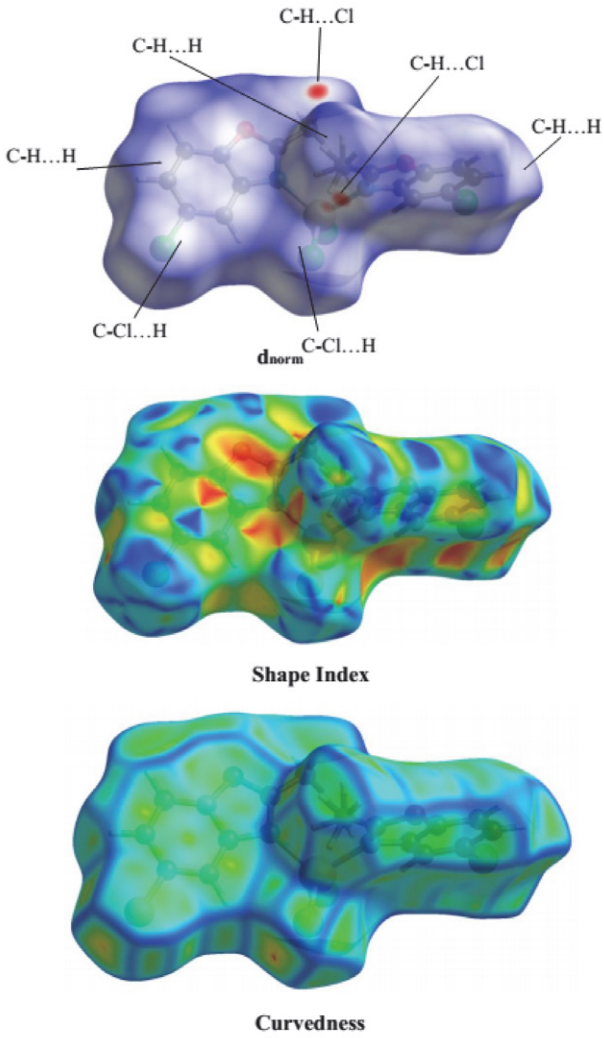

Figure 5: Hirshfeld surfaces mapped with d_{norm}, shape index, and curvedness of zinc(II) complex

(+2). The Hirshfeld surface and 2D fingerprint plots analysis showed various H... Cl/Cl ...H (39.1%), H ... H (21.7%), and H...C/C... H (7.7%) noncovalent interactions are the driving force in stable crystal packing.

Supplementary material

Crystallographic data for the Zin(II) complex have been deposited with the Cambridge crystallographic data Center (CCDC), with the deposit number 2097040. The data can be obtained free of charge via http://www.ccdc.cam.ac.uk/conts/retrieving.html.

Acknowledgments

The authors would like to acknowledge the department of chemistry, college of education, University of Salahaddin and the department of physics, college of science, University of Halabja for providing the required assistance to complete the present study. We acknowledge Nelson Mandela University for single-crystal X-ray diffraction analysis. The authors would also like to thank Mr. Mzgin Ayoob for assisting us with the FT-IR measurement.

Funding

The authors would like to acknowledge the college of science, University of Halabja in Kurdistan region, Iraq for providing the financial funding throughout this study.

5. References

1. D. F. Back, G. M. de Oliveira, M. A. Ballin, V. A. Corbellini, *Inorg. Chim. Acta*. **2010**, *363*, 807–812. **DOI:**10.1016/j.ica.2009.11.033
2. Y. Xu, S. Mao, K. Shen, X. Shi, H. Wu, X. Tang, *Inorg. Chim. Acta*. **2018**, *471*, 17–22. **DOI:**10.1016/j.ica.2017.10.023
3. A. Altun, S. Dursun, N. M. Aghatabay, *Vib. Spectrosc*. **2015**, *81*, 1–12. **DOI:**10.1016/j.vibspec.2015.09.001
4. L. Wang, H. Zhou, J. Wu, Y. Tian, *Dalton Trans*. **2015**, *44*, 9921–9926. **DOI:**10.1039/C5DT01090J
5. Y. X. Sun, W. Y. Sun, *Cryst. Eng. Comm*. **2015**, *17*, 4045–4063. **DOI:**10.1039/C5CE00372E
6. H. Wu, J. Zhang, C. Chen, H. Zhang, H. Peng, F. Wang, Z. Yang, *New J. Chem*. **2015**, *39*, 7172–7181. **DOI:**10.1039/C5NJ01684C
7. M. M. Kimani, D. Watts, L. A. Graham, D. Rabinovich, G. P. Yap, J. L. Brumaghim, *Dalton Trans.* **2015**, *44*, 16313–16324. **DOI:**10.1039/C5DT02232K
8. H. Wu, H. Wang, X. Wang, G. Pan, F. Shi, Y. Zhang, Y. Bai, J. Kong, *New J. Chem*. **2014**, *38*, 1052–1061. **DOI:**10.1039/c3nj01145c
9. K. Zhao, Y. Qu, Y. Wu, C. Wang, K. Shen, C. Li, H. Wu, *Transit. Met. Chem.* **2019**, *44*, 713–720. **DOI:**10.1007/s11243-019-00340-4
10. I. B. Lozada, T. Murray, D. E. Herbert, *Polyhedron*. **2019**, *161*, 261–267. **DOI:**10.1016/j.poly.2019.01.023
11. S. E. Korolenko, K. P. Zhuravlev, V. I. Tsaryuk, A. S. Kubasov, V. V. Avdeeva, E. A. Malinina, A. S. Burlov, L. N. Divaeva, K. Y. Zhizhin, N. T. Kuznetsov, *J. Lumin.* **2021**, *237*, 118156–118169. **DOI:**10.1016/j.jlumin.2021.118156
12. P. Tyagi, R. Srivastava, A. Kumar, V. K. Rai, R. Grover, M. N. Kamalasanan, *Synth. Met*. **2010**, *160*, 756–761. **DOI:**10.1016/j.synthmet.2010.01.016
13. H. B. Zhang, X. F. Zhang, L. Q. Chai, L. J. Tang, H. S. Zhang, *Inorg. Chim. Acta*. **2020**, *507*, 119610–119621. **DOI:**10.1016/j.ica.2020.119610
14. P. H. Santiago, M. B. Santiago, C. H. Martins, C. C. Gatto, *Inorg. Chim. Acta*. **2020**, *508*, 119632119641. **DOI:**10.1016/j.ica.2020.119632
15. I. Habila, M. Saoudi, F. Berrah, B. Benmerad, M. Boudraa, H. Merazig, S. Bouacida, *J. Mol. Struct*. **2021**, *1244*, 130903–130913 **DOI:**10.1016/j.molstruc.2021.130903
16. G. M. Sheldrick, *Acta Crystallogr. A: Found. Adv.* **2015**, *71*,

3–8. **DOI:**10.1107/S2053273314026370
17. C. B. Hübschle, G. M. Sheldrick, B. Dittrich, *J. Appl. Crystallogr*. **2011**, *44*, 1281–1284. **DOI:**10.1107/S0021889811043202
18. L. Krause, R. Herbst-Irmer, G. M. Sheldrick, D. Stalke, *J. Appl. Crystallogr*. **2015**, *48*, 3–10. **DOI:**10.1107/S1600576714022985
19. T. Li, Y. Hu, Opt. Mater. **2020**, *109*, 110260–110264. **DOI:**10.1016/j.optmat.2020.110260
20. L. Q. Chai, Q. Hu, K. Y. Zhang, L. Zhou, J. J. Huang, *J. Lumin.* **2018**, *203*, 234–246. **DOI:**10.1016/j.jlumin.2018.06.058
21. N. S. Abdel-Kader, S. A. Abdel-Latif, A. L. El-Ansary, A. G. Sayed, *J. Mol. Struct*. **2021**, *1223*, 129203. **DOI:**10.1016/j.molstruc.2020.129203
22. E. Al-Masri, M. Al-Refai, H. T. Al-Masri, B. F. Ali, A. Geyer, S. I. Ivlev, N. Aljaar, *Chem. Data Collect*. **2021**, *36*, 100786. **DOI:**10.1016/j.cdc.2021.100786
23. P. Van Thong, N. T. T. Chi, M. Azam, C. H. Hanh, M. Alam, S. I. Al-Resayes, N. Van Hai, *Polyhedron*. **2022**, *212*, 115612. **DOI:**10.1016/j.poly.2021.115612
24. S. V. Larionov, T. F. Kokina, V. F. Plyusnin, L. A. Glinskaya, A. V. Tkachev, Y. A. Bryleva, N. V. Kuratieva, M. I. Rakhmanova, E. S. Vasilyev, *Polyhedron*. **2014**, *77*, 75–80. **DOI:**10.1016/j.poly.2014.04.011
25. N. Ling, X. Wang, D. Zeng, Y. W. Zhang, X. Fang, H. X. Yang, *J. Mol. Struct*. **2020**, *1206*, 127641. **DOI:**10.1016/j.molstruc.2019.127641
26. V. P. Singh, P. Singh, A. K. Singh, *Inorg. Chim. Acta*. **2011**, *379*, 56–63. **DOI:**10.1016/j.ica.2011.09.037
27. K. A. M. I. A. R. Zomorodian, S. O. G. H. R. A. Khabnadideh, *Farmacia*. **2020**, *68*, 155–163. **DOI:**10.31925/farmacia.2020.1.22
28. L. H. Wang, X. Y. Qiu, S. J. Liu, *Acta Chim. Slov*. **2019**, *66*, 675–680. **DOI:**10.17344/acsi.2019.5117
29. R. V. Chikhale, A. M. Pant, S. S. Menghani, P. G. Wadibhasme, P. B. Khedekar, *Arab. J. Chem*. **2017**, *10*, 715–725. **DOI:**10.1016/j.arabjc.2014.06.011
30. A. Jana, B. Das, S. K. Mandal, S. Mabhai, A. R. Khuda-Bukhsh, *New J. Chem*. **2016**, *40*, 5976–5984. **DOI:**10.1039/C6NJ00234J
31. M. Shebl, A. A. Saleh, S. M. Khalil, M. Dawy, A. A. Ali, *Inorg. Nano-Met. Chem*. **2021**, *51*, 195–209. **DOI:**10.1080/24701556.2020.1770794
32. F. Sameri, M. A. Bodaghifard, A. Mobinikhaledi, *Appl. Organomet. Chem*. **2021**, *35*, e6394. **DOI:**10.1002/aoc.6394
33. L. H. Wang, X. Y. Qiu, S. J. Liu, *J. Coord. Chem*. **2019**, *72*, 962–971. **DOI:**10.1080/00958972.2019.1590561
34. Y. Tan, *Acta Chim. Slov*. **2019**, *66*, 1002–1009. **DOI:**10.17344/acsi.2019.5297
35. S. M. Khalil, M. Shebl, F. S. Al-Gohani, *Acta Chim. Slov*. **2010**, *57*, 716–725.
36. P. Singh, D. P. Singh, K. Tiwari, M. Mishra, A. K. Singh, V. P. Singh, *RSC Adv.* **2015**, *5*, 45217–45230. **DOI:**10.1039/C4RA11929K
37. A. Beheshti, M. Bahrani-Pour, M. Kolahi, E. Shakerzadeh, H. Motamedi, P. Mayer, *Appl. Organomet. Chem*. **2021**, *35*, e6173. **DOI:**10.1002/aoc.6173
38. Y. Li, Z. Yang, B. Song, H. Xia, Z. Wang, *Inorg. Nano-Met. Chem*. **2017**, *47*, 966–972. **DOI:**10.1080/24701556.2016.1278554
39. L. Saghatforoush, K. Moeini, S. A. Hosseini-Yazdi, Z. Mardani, A. Bakhtiari, A. Hajabbas-Farshchi, S. Honarvar, M. S. Abdelbaky, *Polyhedron*. **2019**, *170*, 312–324. **DOI:**10.1016/j.poly.2019.05.057
40. L. Saghatforoush, K. Moeini, S. A. Hosseini-Yazdi, Z. Mardani, A. Hajabbas-Farshchi, H. T. Jameson, S. G. Telfer, J. D. Woollins, RSC adv. **2018**, *8*, 35625–35639. **DOI:**10.1039/C8RA07463A
41. Y. Zhang, Y. Q. Pan, M. Yu, X. Xu, W. K. Dong, *Appl. Organomet. Chem*. **2019**, *33*, e5240. **DOI:**10.1002/aoc.5368

Povzetek

Z reakcijo med cinkovim dikloridom in ligandom 5-kloro-2-metilbenzoksazol (L= C_8H_6ClNO) v etanolni raztopini smo sintetizirali nov kompleks Zn(II): dikloridobis(5-kloro-2-metil-1,3-benzoksazol)-cink(II), $C_{16}H_{12}Cl_4N_2O_2Zn$. Spojino smo karakterizirali z elementno analizo, meritvami molarne prevodnosti, FTIR, UVVis in monokristalno rentgensko analizo (XRD). Rentgenska analiza je pokazala, da se v kompleksu kovina in ligand povezujeta v razmerju 1 : 2. Spojina ima popačeno tetraedrično geometrijo z dvema vezanima dušikovima atomoma iz liganda. Izvedli smo izračune z DFT metodo in uporabo B3LYP funkcije z naborom osnov LANL2DZ za kovinski kompleks in 6-31G(d) za nekovinske elemente. Izračunali in predstavili smo optimalno geometrijsko strukturo kompleksa in orbitalne energije HOMO in LUMO. Opravili smo analizo naravnih veznih orbital (NBO) z namenom analize razporeditve naboja pred in po kompleksaciji liganda. Hirshfeldova analiza opravljena na d_{norm} je pokazala da močne medmolekulske interakcije H...Cl/Cl...H in H...H predstavljajo glavni prispevek k pakiranju kristalov.